Journal Homepage: - www.journalijar.com

INTERNATIONAL JOURNAL OF ADVANCED RESEARCH (IJAR)

Article DOI: 10.21474/IJAR01/3272
DOI URL: http://dx.doi.org/10.21474/IJAR01/3272

ISSN NO. 2320-5407

RESEARCH ARTICLE

Synthesis, characterization and oxidase biomimetic catalytic activity of copper(II) complexes with pyridine based ligand containing N_3S_2 donors.

Abd El Motaleb M. Ramadan[1], Asmaa A. Ibrahim[2], Magda A. Barsy[2], Asmaa A. Mostafa[2] and Sami A. Al-Harbi[3].

1. Chemistry Department, Faculty of Science, Kafr El-Sheikh University, Kafr El-Sheikh Egypt.
2. Chemistry Department, Faculty of Science, Aswan University, Aswan, Egypt.
3. Chemistry Department, University College in Al-Jamoum, Umm Al-Qura University, 21955, Makkah, Saudi Arabia.

……

Manuscript Info

Manuscript History

Received: 20 December 2016
Final Accepted: 26 January 2017
Published: February 2017

Key words:-
copper(II) complexes, pyridine based ligand, biomimetic, catalytic activity, phenoxazinone synthase, catechol oxidase.

Abstract

A new series of hexa-, and five- coordinated copper(II) complexes, having the molecular formulae of $[CuLX]X\ H_2O$, **1**, **2**, **3** (X = Cl^-, Br^-, NO_3^-) and $[CuL]X_2\ nH_2O$, **4**, **5** (X= AcO^- and ClO_4^-) respectively and L is pentadentate pyridine based ligand have been synthesized. Structural characterization of these newly synthesized compounds was achieved by several physicochemical methods including elemental and thermal analysis (TGA and DTG), electrical molar conductance, magnetic moment measurements and spectral investigations such as IR, UV-Vis and ESR. The spectral and magnetic measurements in addition to the electrolytic conductance results demonstrated the octahedral and square-pyramidal stereochemistries for the hexa, and five coordinated copper(II) chelates respectively. Catechol oxidase and phenoxazinone synthase biomimetic catalytic activity of the inspected copper(II) chelates was studied and the results obtained indicated that, the catalytic reactivity is markedly depends on the structural properties of these newly synthesized copper(II) complexes.

Copy Right, IJAR, 2017,. All rights reserved.

……

Introduction:-

Functional models of the metalloenzymes that activate molecular oxygen possess great potential as catalyst for specific oxidation reactions and as guides for the development of efficient small molecule catalysts [1]. Since, the oxidation of organic substrates with molecular oxygen under mild conditions is of great interest for industrial [2] and synthetic processes both from an economical and environmental [3] point of view, most of the focus of ongoing biomimetic and bioinspired synthetic approaches is on reproducing some structural and/or functional feature of the title enzymes. The synthesis and reactivity studies of transition metal complexes, as functional model compounds for metalloenzymes with oxidase activity, are of particular interest for the development of bioinspired catalysts for oxidation reactions.

The potential role played by copper ions in the active sites of a large number of metalloproteins has stimulated efforts to design and characterize copper complexes as models for providing better understanding of biological systems and for assisting in the development of new homogeneous catalysts for selective oxidation. Particularly, the coordination chemistry and reactivity of copper complexes involving nitrogen–sulfur donor ligands has received considerable attention as models [4]. In particular the CuN_2S_2 chromophore is present in blue copper proteins such as plastocyanin [5] and copper(II) chelates of SNNS ligands have been found to have antineoplastic activities and to interact with biological systems [6].

Oxidase or dehydrogenase enzymes catalyze the oxidation of substrate by employing dioxygen as a hydrogen acceptor *e.g.* copper containing oxidase, e. g. catechol oxidase and phenoxazinone synthase. Catechol melanin, a black pigment of plants, the black color of banana and black sugar, is a polymeric product formed by the oxidative polymerization of catechol [7]. Another type of catechol oxidase, this copper(II) protein isolated from photogenic materials, only catalyzes the oxidation of catechol to quinones without acting on tyrosine [8,9]. Catechol oxidase forms the third member of Cu / O_2 group which belongs the type III copper protein [10,11]. Catechol oxidase in contrast to tyrosinase, catalyze exclusively the oxidation of catechol to the corresponding *o*-quinones without acting on monophenols [12]. This reaction is of great importance in the medical diagnosis for the determination of hormonal catecholamine (adrenaline, noradrenalin and dopamine).

Related to catechol oxidase is phenoxazinone synthase, it is a type 2 copper containing oxidase (subunit molecular mass 88000 3.7 Cu per subunit) [13] is naturally found in the bacterium Streptomyces antibiotics and has been cloned and over expressed in *S. lividians* [14]. It is an oligomeric multicopper oxidase, catalyses the oxidative coupling of two molecules of an *o*-aminophenol to form the phenoxazinone chromophore. This reaction constitutes the final step in the biosynthesis of actinomycin and is a complex six-electron oxidative condensation.

In continuation of our earlier work in the area of copper(II) chemistry we describe here in this contribution the synthesis and characterization of a new series of copper(II) complexes containing the pentadentate neutral pyridine base ligands, as potential structural and functional models for the active sites of both catechol oxidase and phenoxazinone synthase.

Experimental:-

Materials:-

All chemicals used were of analytical grade. The benzoyl hydrazine, hydrazine hydrate 95%, 2,5-dibromo methylbenzene and 2,6-dibromo methyl pyridine were purchased from Aldrich. 2,3-Dibromo methyl quinoxaline was synthesized based on the method reported in literature [15]. Phenyl triazole was prepared according to the modified method described below.

Preparation of phenyl triazole:-

CS_2 (0.15 mole) was added drop wise to an ice cold solution of KOH (9.12 gm, 0.16 mol) in absolute ethanol (200 ml) containing benzoyl hydrazine (0.1 mol). The reaction mixture was diluted with ethanol (150 ml) and stirred for 2h at room temperature. Dry ether (200 ml) was added and the resulting solid K-salt precipitate was collected, washed with ether and finally dried.

A solution of the latter K-salt (0.05 mol) and hydrazine hydrate 95 % (0.5 mol) was heated under reflux with stirring for one hour. 5 ml of water was then added and the reaction mixture was neutralized with concentrated hydrochloric acid. The solid obtained upon neutralization was collected and crystallized from acetic acid to give colorless crystals of phenyl-triazole (mp. 214-216 °C).

Preparation of the pyridine based ligand (L) :-

To a solution of phenyl triazole (50 mmol) in aqueous ethanol (50 ml) containing KOH (50 mmol) the appropriate dibromo compounds (25 mmol) was added. The reaction mixture was heated under reflux for 1 h. The solvent was then removed in vacuum and the remaining solid was collected and crystallized from DMF to give colorless crystals of the product ligand pyridine based ligand L.

Synthesis of copper(II) complexes 1-5:-

An equimolar amount of copper(II) salt in 25 ml ethanol was added drop wise to a 25 ml hot ethanolic solution of the organic ligand (L). The reaction mixture was stirred for half hour at room temperature. The resultant reaction mixture was further stirred under reflux for one hour during which time colored products precipitated. After that, the volume of the solution of the reaction mixture was reduced, then filtered and the isolated solid was washed with ethanol and ether and finally dried in *vacuum* over CaO at room temperature for several days.

Physical measurements:-

IR spectra were recorded using KBr disks in the 4000-200 cm^{-1} range on a Unicam SP200 spectrophotometer. The electronic absorption spectra were obtained in DMF solution with a Shimadzu UV-240 spectrophotometer. Magnetic moments were measured by Gouy's method at room temperature. ESR measurements of the polycrystalline samples at room temperature were made on a Varian E9 X-band spectrometer using a quartz Dewar vessel. All spectra were calibrated with DPPH ($g = 2.0027$). The specific conductance of the complexes was measured using freshly prepared 10^{-3} M solutions in electrochemically pure DMF at room temperature, using an YSI Model 32 conductance meter. The thermogravimetric measurements were performed using a Shimadzu TG 50-Thermogravimetric analyzer in the 25-1000 °C range and under an N_2 atmosphere. Elemental analyses (C, H, and N) were carried out at the Micro analytical Unit of Cairo University.

Oxidase biomimetic catalytic activity:-

A mixture of 1.0 ml of studied substrate 3,5-di-*tert*-buty1catehol (3,5-DTBCH_2) or 2-aminophenol (2-APH) solution (30 mM) in methanol and 1.0 ml of copper complex solution (~3 mM) in methanol was placed in a 1 cm path length optical cell containing 1.0 ml of methanol in a spectrophotometer. The final concentration of reaction mixture is catechol or 2-aminophenol (10 mM) and complex (l mM). The formation of 3,5-di-*tert*-butyl-quinone (3,5-DTBQ) was followed by observing the increase of characteristic quinone absorption band at 400 nm and for 2-amino-3*H*-phenoxazine-3-one (APX) at 433 nm.

Results and discussion:-

Synthesis and characterization of L and copper(II) complexes:-

The reported ligand L (Figure 1) was prepared as previously reported in the experimental section and characterized by IR, elemental analysis, and UV–Vis spectra. Reaction of the present pyridine based ligand, L with copper(II) salts (CuX_2; X = Cl^-, Br^-, NO_3^-, AcO^- and ClO_4^-) in a 1:1 ratio in ethanol gives a new series of copper(II) complexes having the molecular formulae of [CuLX]X (X = Cl, Br, NO_3) and $[CuL]X_2$ (X = AcO and ClO_4). The elemental analyses are consistent with the proposed molecular formulae that show the ratio of metal/ligand is 1:1. The molar conductivities of 10^{-3} M solutions of these copper(II) chelates in DMF at 25 °C are measured and the data obtained are listed in Table 1. These electrolytic conductance results reveal that the halogeno and nitrato copper(II) complexes have molar conductivity values in the range 63.67 – 88.16 Ω^{-1} mol^{-1} cm^2, which indicates their ionic nature and they are considered as 1:1 electrolytes [16]. These molar conductance values indicate the hexa coordinate formulation of these halogeno and nitrato copper(II) complexes in an octahedral structure. On the other hand the acetate and perchlorate complexes exhibit molar conductance values of 143.85 and 149.19 Ω^{-1} mol^{-1} cm^2, respectively demonstrating that they are 1:2 electrolytes and suggest the five-coordinate formulation of these complex species. Thus the pyridine based ligand L must act as a neutral pentadentate chelating ligand in complexation to copper(II) ion. On the basis of the elemental analyses, and the molar conductance measurements the complexes were assigned the compositions shown in Table 1.

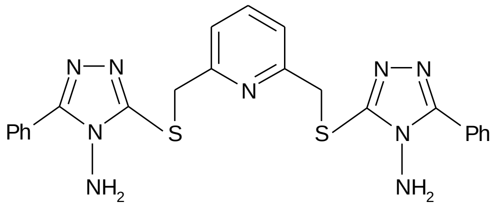

Fig. 1. Structure of the pyridine based ligand (L)

Table 1. Molecular formulae, physical properties and analytical data of copper(II) complexes **1-5**

Complex	Color	Λ_M (Ω^{-1} cm^2 mol^{-1})	Found (Calcd.) %C	%H	%N	%M
1. $[CuL^1Cl]Cl\ H_2O$	Faint green	95.30	43.16(43.29)	3.63(3.29)	18.95(19.77)	10.57(9.96)
2. $[CuL^1Br]Br.H_2O$	Faint brown	93.67	37.67(37.98)	3.18(2.89)	16.85(17.35)	9.11(8.74)
3. $[CuL^1NO_3]NO_3\ H_2O$	Fain blue	98.16	40.59(39.96)	3.37(3.04)	21.45(22.31)	9.94(9.20)
4. $[CuL^1](AcO)_2\ H_2O$	Fain blue	143.85	47.50(47.33)	4.15(3.94)	17.92(18.41)	10.05(9.28)
5. $[CuL^1](ClO_4)_2$	Green	145.19	37.62(36.92)	2.79(2.54)	16.31(16.86)	09.89(8.49)

Thermal analysis:-

Thermal decomposition (TGA and DTG) studies:-

The thermal decomposition studies on the synthesized copper(II) complexes have been carried out so as to corroborate the information obtained from their molar conductance and spectral studies about the statues of water molecules present in these complexes, as well as to know their general decomposition patterns. Due to the explosion nature of the perchlorate anion the perchlorate complex was ruled out from the thermal studies. The decomposition stages, temperature ranges, maximum decomposition peak DTG_{max}, percentage mass losses of the decomposition reactions together with their theoretical percentage mass losses and the assignments of decomposition moieties are given in Table 2, which reveals the following findings.

The thermograms (TG and DTG curves) of the hydrated copper(II) complexes $[CuLCl]Cl.H_2O$, $[CuLBr]Br.H_2O$, $[CuLNO_3]NO_3.H_2O$ and $[CuL](AcO)_2\ H_2O$, show a similar decomposition patterns. Three successive overlapped and unresolved degradation stages within a temperature range 60 - 700 °C are observed. The first stage of thermal decomposition starts at 65 °C and is marked with a regular loss in mass up to 120 °C. The initial mass loss for the complexes varies from 2.53 to 3.15 %, and agrees well with the theoretical expected mass loss of 2.60 – 3.63%. This is mainly due to the dehydrate removal of the out sphere water molecules (the adsorbed, crystalline or lattice water). The maximum rate of mass loss occurs at a temperature range of 85 - 105 °C as indicated from the DTG peaks. The activation energy of this thermal dehydration step is 14.06 – 30.25 $kjmol^{-1}$ (Table 3). This ease of desolvation suggests the weak interaction of and indicates that water plays little or no role in the lattice forces and occupies crystal voids.

The second stage of mass-loss reveals that the formed anhydrous complex species are then further decomposed within the temperature range 110 – 280 °C, with DTG maximum peaks at 140 - 240 °C range. This process corresponds to the volatilization of the loosely bonded non-coordinated electrolytic counter anions with a mass loss of (6.12 – 17.10 %) in accordance with the calculated values of (5.57 – 17.23 %). The energy values of activation of this stage lay in the range 25.23 – 75.24 $kjmol^{-1}$ (Table 3).

The third stage involves a significant mass loss extending in the temperature range from 190 to 675 °C with DTG_{max} peaks at 250 - 620 °C range ascribed to the exothermic removal of the axially coordinated counter anions namely, Cl^{-}, Br^{-} and NO_3^{-} in addition to the complete burning of the organic ligand molecule in successive steps, leaving behind metal oxide as the final product of the thermal pyrolysis of the complex molecule. A good agreement between the experimental and calculated values is reported for the mass loss (Exp. 63.94 - 77.63 %; Calcd. 63.81 - 78.38 %), and the associated activation energy values are in the range 30.95 – 65.85 $kjmol^{-1}$. Further horizontal constant curve may be due to the presence of metal oxide residue in the remaining part. The total loss of weight agrees well with the corresponding calculated data and the final product is anhydrous CuO. For all complexes, the metal content, determined from the oxide residue, was found to be satisfactory agreement with values calculated on the basis of the suggested composition formulae based on the analytical data.

Table 2. Thermogravimetric analysis of copper(II) complexes

*Complex	Temperature °C	DTG_{max} °C	% Weight loss Found (Calcd.)	Species formed
1	75 – 110	85	3.15(2.82)	$[CuL^1Cl]Cl$
	110 – 280	240	6.12(5.57)	$[CuL^1Cl]$
	280 – 530	280, 500	77.63(78.38)	CuO
2	90 – 110	105	2.53(2.77)	$[CuL^1Br]Br$
	110 – 220	200	11.23(11.01)	$[CuL^1Br]$
	220 – 345	250	11.05(11.01)	$[CuL^1]$
	345 – 500	340, 440	63.94(63.81)	CuO
3	65 – 120	90	2.72(2.60)	$[CuL^1(NO_3)]NO_3$
	120 – 190	175	9.15(8.99)	$[CuL^1(NO_3)]$
	190 – 570	250, 545	75.91(75.97)	CuO
4	60 – 110	85	2.45(3.63)	$[CuL^1](AcO)_2$
	110 – 280	140	17.10(17.23)	$[CuL^1]$
	280 –675	225, 620	68.00(67.56)	CuO

*Complex details are as listed in Table 1.

Thermal Kinetic Studies:-

The thermodynamic parameters of the decomposition processes of the inspected copper(II) complexes, namely, activation energy (E_a), enthalpy (ΔH), entropy (ΔS), and Gibbs free energy change (ΔG) were evaluated graphically by employing the Coats-Redfern equations [17] and the data obtained are given in Table 3.

The data in Table 3 show that, the values of the activation energies of the investigated copper(II) chelates reflect the thermal stability of these complexes. The activation energy values (E_a) of the removal of the electrolytic non-coordinated counter anions are lower than the subsequent stages of thermal degradation of these complexes. This finding indicates that the electrolytic counter anions are loosely bond to copper(II) center and confirms the presence of one of the two counter anions outside the coordination sphere. In contrary the activation energy values (E_a) associated to removal the non-electrolytic coordinated counter anions are higher than that reported for decomposition stage of electrolytic counter anions. This results demonstrate incorporation two types of counter anions in complex molecule and confirm the suggested compositional formulae of these copper(II) chelates. The ΔG values of the thermal decomposition of the present copper(II) complex species increase for the subsequently decomposition stages due to increasing the values of $T\Delta S$ from one step to another. This observed trend in the values of ΔG reflects that the rate of the removal of the counter anion ligands is lower than that of the precedent organic ligand. This finding may be ascribed to the structural rigidity of the original complex molecule as compared to the resultant intermediates formed during the thermal pyrolysis processes.

On the other hand the activation energy values of the first stage which describes dehydration (surface or lattice water) are lower than that of the subsequent stages of thermal degradation of these complexes. This may attributed to the less steric strain in the intermediate compounds obtained after the first stage of the thermal pyrolysis. It is noteworthy to note that the removal of the electrolytic counter anion and the crystalline or surface water content of the complex molecule have lower ΔH values than the removal of coordinated counter anion and the organic moiety of the coordinated ligand to yield the CuO as a final product.

Table 3. Kinetic and thermodynamic parameters of copper(II) complexes

*Complex	T° (K)	*A*	E_a	ΔH	ΔS	ΔG
1	380	5.690	18.41	15.49	-0.2599	114.26
	514	4.850	25.23	22.31	-0.2637	157.88
	723	3.400	30.95	28.03	-0.2695	222.91
2	388	10.57	14.06	43.14	-0.2358	136.63
	503	16.15	46.68	45.76	-0.2424	165.72
	073	19.71	114.53	111.61	-0.2338	245.61
3	373	4.20	27.13	24.21	-0.2435	115.04
	433	5.98	47.45	44.53	-0.2125	177.53
	523	19.10	83.41	80.49	-0.2543	212.54
4	373	5.16	30.25	27.33	-0.2414	117.38
	445	12.61	75.24	72.33	-0.2374	147.41
	528	9.99	83.74	80.82	-0.2369	166.47

*Complex details are as listed in Table 1. E_a, ΔH and ΔG are in kJ mol^{-1}, ΔS in J mol^{-1}.

IR spectral studies:-

The most relevant IR bands and proposed assignments for the organic ligand and its copper(II) complexes are listed in Table 4. All compounds under study give normal infrared spectra with vibrations characteristic for the ligand system and the counter anions present in the complex molecule. The IR spectra of the inspected complexes are compared with the free ligand in order to determine the coordination sites that may be involved in chelation. In the IR spectrum of the free ligand the significant bands are observed at 3247 cm^{-1} for $\upsilon(NH_2)$, 1440 for ring skeletal vibrations $\upsilon(C{=}C)$, 765 cm^{-1} for $\upsilon(C–S)$, 1554 cm^{-1} for $\upsilon(C{=}N_{pyridine})$ and $\delta(NH_2)$ at 1240 cm^{-1}. Upon complexation these bands are shifted to higher or lower wave numbers in the spectra of complexes. The shift in band position of these characteristic functional groups is an indication of the participation of nitrogen atoms of both the primary amine, and the pyridine ring in addition to the two sulfur atoms of the ligand system in coordination to the copper(II) ions [18]. However, the IR spectra of all complexes are very similar and besides what has been noted above, exhibit medium to strong bands at *ca*. 1565 - 1579 cm^{-1} as expected for the high energy ring vibrations of the coordinated pyridine. The bonding of the pyridine nitrogen atom is also shown by the presence of bands at 1010-1035 cm^{-1} and 630 - 668 cm^{-1} attributable to the ring breathing frequency and the low energy pyridine ring vibrations, respectively

[19]. Therefore, from the IR spectra, it is concluded that the reported ligand behaves as neutral pentadentate in all the complexes and coordinates to the metal ion *via* the pyridyl nitrogen, the two nitrogen atoms of the primary amine groups and the two sulfur atoms of the ligand system. The low frequency bands in all the complexes in the region 535 – 570 cm^{-1} and 421 – 455 cm^{-1} are assigned to υ(Cu–N) and υ(Cu–S), respectively and provide a compelling evidence for the presence of metal– nitrogen and metal- sulfur bond in the complexes molecules [20,21]. For all complexes medium to strong bands present in the region around 4500 cm^{-1}, assignable to *υ*(OH), clearly confirm the presence of surface or lattice water. Since vibrational modes such as wagging, twisting and rocking activated by coordination to the metal have not been found in the expected ranges, it appears that coordinated water is not present. These results are consistent with the thermogravimetric studies, using TG and DTG techniques; in fact this water is lost in the 60 – 110 ºC range.

The appearance of a broad absorption band centered on 4500 cm^{-1} in the spectra of these hydrated complexes, indicate the presence of lattice water. The band at 3247 cm^{-1} is assigned to the amino group stretching vibration in the free ligand. The presence of stretching vibration of the water molecules in the spectra of these complexes renders it difficult to confirm the participation of the amino group in chelate formation of these hydrated complex species. The participation of the NH_2 group is inferred and confirmed by clarifying the effect of chelation on the in-plane bending, $\delta(NH_2)$ vibration. The shift of this band, from 1240 cm^{-1} in the free ligand L, to 1219 –1229 cm^{-1} in the spectra of these hydrated complexes indicates the participation of the NH_2 group in complex formation [18].

In addition to showing the characteristic bands due the coordinated organic ligand the spectra of the present copper(II) complexes also show the characteristic frequencies of the counter anions (electrolytic and nonelectrolytic) incorporated in the complex molecule. Regarding the nitrato complex the asymmetrical stretching frequency for the nitrate ion υ_3 are observed at 1304 cm^{-1} and 1418 cm^{-1} and the υ_1 vibration at 841 cm^{-1}. These results signify a monodentate mode of nitrate binding [22]. Moreover two strong bands at 1420 – 1430 and 1306 – 1312 cm^{-1} at a separation of 114 – 118 cm^{-1} indicate that the nitrate is bound in monodentate fashion [22]. On the other hand the weak band observed at 725 and 720 cm^{-1} may be assigned to υ_2 of the uncoordinated nitrate ion. These spectral features suggest that this nitrato complex contains both the non-electrolytic coordinated monodentate nitrate ligand and the electrolytic nitrate ion [18,23].

The spectrum of the perchlorate complex exhibits the strong, unsplit absorption band, centered at 1085 – 1104 cm^{-1}, characteristic of non-coordinated perchlorate. The non-coordination and the electrolytic ionic nature of the acetate ion was inferred from the strong bands occur at 1680, 1258 and weak band at 412 cm^{-1}. These results are in harmony with the electrolytic conductance measurements of the complexes in DMF at 25 °C where the molar conductance values for the perchlorate and acetate complexes lie in the range characteristic of 1:2 electrolytes. For the hexa-coordinated halogeno complexes, the non-electrolytic halide ion exhibits weak absorption band far infra red region characteristic of the axially coordinated halide ion [25].

On the basis of the above discussion the general structures have been proposed for the present copper(II) complexes as shown in Figure 1.

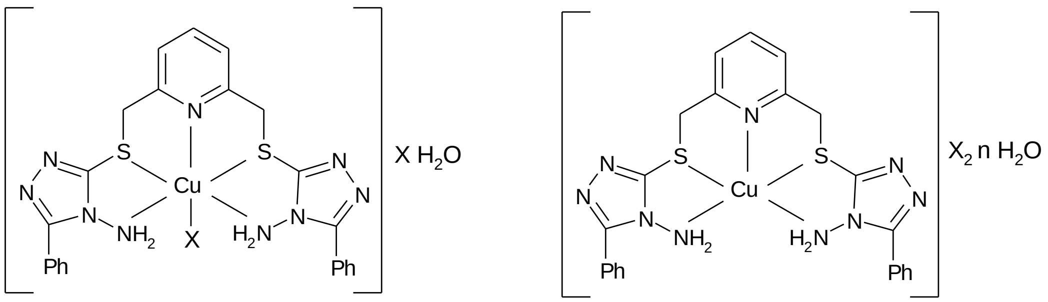

For complex **1**, X = Cl,
complex **2**, X = Br,
complex **3**, X = NO_3

For complex **4**, X = CH_3COO^-, n = 1
complex **5**, X = ClO_4, n = 0

Fig. 2. Structure of copper(II) complexes

Table 4. Infra red spectra of pyridine based ligand (L) and its copper(II) complexes.

*Compound	υ(H_2O)	υ(py)	δ(NH_2)	ring breathing	υ(C-S)	δ(py)	υ(N-Cu)	υ(S-Cu)
L	**3247	1554	1240	1010, 630	765	684	-	-
1	4530	1569	1219	1029, 655	773	680	521	415
2	4540	1575	1223	1025, 649	775	690	517	420
3	4529	1565	1227	1030, 660	787	686	519	420
4	4533	1579	1225	1027, 658	779	655	515	450
5	**3223	1570	1229	1035, 668	785	686	525	452

*Complex details are as listed in Table 1. **Characteristic band of υ(NH_2)

Electronic absorption spectra:-

The electronic absorption spectra of the inspected ligand and its copper(II) complexes were recorded in DMF solution and the results obtained are given in Table 5. The spectrum of the present ligand (L) exhibits two major peaks. The first one peak at 34482 cm^{-1} is assignable to $\pi \rightarrow \pi^*$ transitions of the aromatic ring. The second band at 30769 cm^{-1} is attributed to the $n \rightarrow \pi^*$ transition of the –C=N− function in pyridine ring of this ligand system [26].

In the high energy region, the electronic absorption spectra of a 10^{-3} M solution of the newly synthesized copper(II) complexes in DMF show two major absorption bands in the range 34482 – 34105, 29171 – 28069 cm^{-1} range for the first and second peaks respectively in addition to a shoulder at 25188 - 26315 cm^{-1} range. The first peak is assigned to $\pi \rightarrow \pi^*$ intraligand transitions. This band is at some what the same frequency in the free ligands L, which tells us that these transitions are not significantly affected by chelation. The extensive π conjugation present in these ligand systems clearly creates an environment for this type of intraligand $\pi \rightarrow \pi^*$ transitions [27]. On the other hand the second band is corresponding to the –C=N− group in pyridine ring showed an observable shift to longer wavelength on going from ligand to complex, indicating coordination of ligand to metal enter through the azomethine moiety [28]. The detected shoulder at the range of 25188 - 26315 cm^{-1} could be due to Cu(II) → ligand charge transfer (MLCT) transitions [29a]. The observed band in the 26306 – 27472 cm^{-1} region is assigned to $S \rightarrow Cu^{II}$ (LMCT) transition. The presence of the $S \rightarrow Cu^{II}$ (LMCT) band in the spectra of all complexes is strong evidence that coordination of the reported ligand to the metal ion occurs *via* the sulfur atom [29b]. Such LMCT bands are quite common in the electronic spectra of related copper(II) complexes containing sulfur donors [30].

The electronic absorption spectra of the investigated hexacoordinated copper(II) complexes, **1**, **2** and **3** at 10^{-3} M of complex concentration in DMF show one d-d band at around 550 nm in the form of one broad band envelope which can be assigned to $^2E_g \rightarrow {}^2T_{2g}$ transition of an octahedral geometry. Though in cases where the ^2E_g and $^2T_{2g}$ states of the octahedral copper(II) ion (d^9) split under the influence of the tetragonal distortion the three transitions $^2B_{1g} \rightarrow {}^2E_g$, $^2B_{1g} \rightarrow {}^2B_{2g}$, and $^2B_{1g} \rightarrow {}^2A_{1g}$ are expected [31], their very close energies could have made them appear as an one broad band envelope. To overcome this difficulty we used saturated solution of metal complexes for measuring the electronic absorption spectra in the low energy region i. e. in the visible and the IR region. Therefore, we have succeeded to detect three d-d bands at wave number (cm^{-1}) ranges of 20278 – 21418 and 16989 – 17723 and a shoulder band at 14061 – 14184 cm^{-1} range corresponding to the above said transitions, $^2B_{1g} \rightarrow {}^2E_g$, $^2B_{1g} \rightarrow {}^2B_{2g}$ and $^2B_{1g} \rightarrow {}^2A_{1g}$ respectively in a distorted octahedral geometry (Table 5).

For the inspected hexacoordinated copper(II) complexes, since the planner field and one of the axial field are constant in all these copper(II) complexes, the change in the d-d band's frequency should be due to nature of the other donor set of the axial field. The electronic absorption spectral features of these six coordinate copper(II) complexes reveal that the position and intensity of the d-d bands are sensitive to the nature of the counter anion occupies the axial plane of the octahedral stereochemistry. Thus, the relative energies of the d-d transition will depend upon the extent of the axial ligand-metal interaction. For a given ligand L, the data in Table 5 show that the increasing energy order of the d-d band lies in the sequence: $CuLNO_3$ < CuLBr < CuLCl and reflects the decreasing order of the Lewis-acidity of the central copper(II) ion. This finding suggests that the strength of the metal-axial counter anion ligand bond increases in the order of NO_3 < Br < Cl.

The data in Tables 5, show that, the electronic absorption spectral features for the inspected five–coordinated copper(II) complexes **4** and **5** are similar. Three weak bands appearing in the low energy visible region at 15057 – 15317, 17104 – 17384 and 20755 – 20982 cm^{-1} ranges may be attributed to the d–d transitions of the copper(II) ion in the square-pyramidal environment (C_{4v}) [32]. In the square – pyramidal copper(II) complexes the plausible d-orbital energy level scheme (idealized symmetry group C_{4v}), is $dx^2–y^2 > dz^2 > dxy > dxz, dyz$. Accordingly, for the investigated perchlorate and acetate copper(II) complexes the higher energy band of the d-d transitions can be assigned to d_{xz}, $d_{yz} \rightarrow dx^2–y^2$, $d_{xy} \rightarrow dx^2–y^2$ while the lower energy band to $dz^2 \rightarrow dx^2–y^2$. These spectral parameters are in consistence with the other copper(II) complexes in the five-coordinate square-pyramidal stereochemistry [31,33,34]. This finding is further confirmed from the results of the ESR spectra.

Table 5. Electronic absorption spectra pyridine based ligand and its copper(II) complexes

			$\lambda(cm^{-1})$			
*Complex	$^2B_{1g} \longrightarrow {}^2A_{1g}$	$^2B_{1g} \longrightarrow {}^2B_{2g}$	$^2B_{1g} \longrightarrow {}^2E_g$	$S \rightarrow Cu^{II}$	$n \rightarrow \pi^*$	$\pi \rightarrow \pi^*$
L					30769	34482
1	14184	17723	21418	27472	28102	34413
2	14154	17447	20840	26737	28171	34482
3	14071	16989	20658	26173	28005	34398
	$dz^2 \rightarrow dx^2–y^2$	$d_{xy} \rightarrow dx^2–y^2$	$d_{xz}, d_{yz} \rightarrow dx^2–y^2$			
4	15236	17104	20982	26666	29069	34365
5	15317	17314	20755	26315	29018	34413

*Complex details are as listed in Table 1.

ESR spectra and magnetic moment measurements:-

As further structural characterization tools, the magnetic moment measurements and the ESR spectra studies have been used to confirm the geometry of the reported copper(II) complexes. Copper (II) ion belongs to the $3d^9$ and $S = 1/2$ system [35,36]. The room temperature magnetic moments and details of the polycrystalline ESR spectra of the studied copper(II) complexes are listed in Table 6. The observed magnetic moments of the investigated copper(II) complexes lie in the 1.95 - 2.12 BM range, corresponding to one unpaired electron [35,36] and in consistence with the mononuclear monomeric structure of these complexes. Based on these normal magnetic moment values, there seems to be no exchange interaction between the copper(II) ions in the solid state of these copper(II) chelates. This fact finds support from the ESR spectral data which give G values in the range 5.3825 – 6.9749 > 4.0 [37].

The EPR spectra of the inspected copper(II) complexes in the polycrystalline state at 298 K were recorded in the X-band region, using 100 KHz field modulation and the g factors; $g_{||}$ and $g_{\perp}$ values were quoted from the spectra relative to the standard g-marker DPPH ($g = 2.0023$). The spectra are interpreted in term of an effective spin of $S = 1/2$, and the various ESR parameters $g_{||}$, $g_{\perp}$, G and g_{av} computed from these spectra are given in Table 6. The spectra of most complexes show one signal at $g_{av} = 2.0920 - 2.1276$ and no hyperfine structures were observed. This finding may be attributed to the strong dipolar interaction between the copper(II) ions in the unit cell. However, the spectra of the present six and five coordinate complexes species are anisotropic, having parallel and perpendicular features.

The ESR spectra of the investigated hexa-coordinate copper(II) complexes **1**-**3** show a considerable tetragonal distortion occurs, which changes the symmetry of O_h to D_{4h}. According to the Jahn-Teller thermo, a tetragonal distortion reduces the symmetry from O_h to D_{4h} [36] is expected for all hexa-coordinate copper(II) complexes and this results in an anisotropy of the g-tensor. For the six coordinated copper(II) complexes under study the coordinated donors are not identical, where the coordination chromophore is N_3S_2X therefore, only static distortion can occur [36]. However, the solid state EPR spectra of these complexes, recorded at ambient temperature were found to be anisotropic with g-values, $g_{||} = 2.2040 – 2.2748$ and $g_{\perp} = 2.0326 - 2.0425$ (Table 6). The spectra are axial in nature and $g_{||} > g_{\perp} > 2.0023$, indicating that $dx^2–y^2$ is the ground state, which is characteristic of a distorted octahedral geometry [38]. The value of $g_{||}$ is greater than $g_{\perp}$ (Table 6) indicating a tetragonal distortion, corresponding to elongation along the four-fold symmetry Z axis. The g_{av} value calculated from the relation: $g_{av} = 1/3(g_{||} + 2g_{\perp})$ was found to lie in the range 2.0920 - 2.1196. The deviation of the g_{av} from that of the free electron (2.0023) is due the covalent nature [39]. This covalent planar bonding like other complexes of sulfur and nitrogen donor ligands is supported by a $g_{||}$ values of 2.2040 – 2.2748 range as suggested by Kivelson and Neiman [40]. The parameter G has been calculated by using the expression [41]: $G = (g_{||} - 2)/(g_{\perp} - 2)$. The value of G reflects the exchange interaction between copper centers in the polycrystalline complex. According to Hathaway et al. [42] values of G less than 4 indicate considerable exchange interaction in the solid complexes while values of G larger than 4 are typical of negligible exchange interactions, which is the case in the copper(II) complexes under investigation.

The one-electron paramagnetic of the five–coordinated copper(II) complexes $[CuL](CH_3COO)_2$ (**4**) and $[CuL](ClO_4)_2$ (**5**) display axial X-band EPR spectral features that are characteristic for an essentially square pyramidal geometry giving $g_{||}$ and $g_{\perp}$ values of 2.2504 - 2.2913 and 2.0359 – 2.0458 range respectively, at 293 K. Both $g_{||}$ and $g_{\perp}$ values are within the range expected for square pyramidal or tetragonal copper(II) complexes. The fact that $g_{||} > g_{\perp}$ is consistent with a $dx^2–y^2$ ground state for what is probably a distorted square pyramidal disposition of atoms about the central copper ion [43]. Here also the $g_{\|}$ value is less than 2.3, indicating the covalent character of M−L bonds [40]. For these complexes the value of *G*-factor is greater than 4, suggesting that there is no interaction between the copper centers. The small separation between the $g_{\|}$ and the $g_{\perp}$ lines indicates that the unpaired electron on copper may be significantly delocalized into the ligand system. A pathway for electron delocalization is provided by the pyridine entity directly linked to the copper ion by the nitrogen atom through overlap of d orbitals of copper with the N system of pyridine.

Table 6. ESR spectral parameters and magnetic moment values of copper(II) complexes

*Complex	$g_{\|}$	$g_{\perp}$	g_{av}	*G*	μ_{eff} (BM)
1	2.2748	2.0425	2.1196	6.4650	2.12
2	2.2110	2.0326	2.0920	6.4723	2.04
3	2.2040	2.0379	2.0932	5.3825	1.95
4	2.2913	2.0458	2.1276	6.3602	1.97
5	2.2504	2.0359	2.1074	6.9749	2.05

*Complex details are as listed in Table 1.

Oxidase Biomimetic Catalytic Activity:-

There is a continuing interest in the biomimetic catalytic activity of the transition metal complexes, which may serve as structural and functional models for various metalloenzymes [44]. In the modeling approach metalloenzymes are regarded as metal complexes embedded in the protein structure. It is therefore convenient to investigate the low molecular mass complexes with the objective of obtaining structural information on the reactivity patterns transferable with the same reservation to the enzyme [45]. We are interested in the modeling of the metalloenzymes catechol oxidase and phenoxazinone synthase. These enzymes play vital roles in the metabolism of the aromatic compounds.

Catechol oxidase biomimetic catalytic activity:-

Catechol oxidase is a copper type two enzyme catalyzes the aerobic oxidation of catechol to the corresponding light absorbing *o*-quinone. The two-electron oxidation of 3,5-di-*tert*-butyl catechol (3,5-DTBCH_2) to the light absorbing 3,5- di-*tert*-butyl quinone (3,5-DTBQ) was investigated since this is the reaction that the copper-containing enzyme catechol oxidase catalyzes (Figure 3).

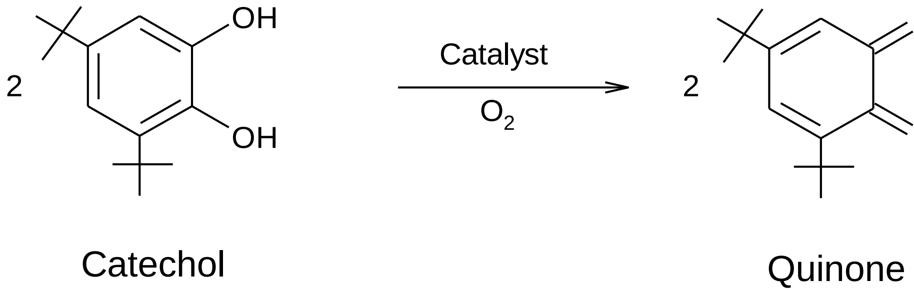

Fig. 3. Catalytic aerobic oxidation of 3,5-di-*tert*-butylcatechol

The catechol oxidase biomimetic catalytic activity of the reported copper(II) complexes was evaluated by determining the turn over rate (amount of 3,5-DTBQ produced per min per mg of catalyst) by making use of molar absorbance value of ε = 1900 M^{-1} cm^{-1} in methanol and the obtained results are given in Table 7. As we can seen in Table 7, all the inspected complexes catalyze the aerobic oxidation of 3,5-DTBCH_2 to the corresponding light absorbing 3,5-DTBQ with the oxidase like catalytic activity varying from a relatively high for **3** to a moderate for **4** and **5** and a low for **1** and **2** complexes. These results demonstrate that, the catalytic activities depend strongly on the nature of both the counter anion incorporeities in the complex molecule and the stereochemistry of the metal chelate. There are a number of factors that could help to elucidate the difference in the catalytic activates of the present catechol oxidase functional models. These include:

(a) The redox potential of the couple Cu^{I}/Cu^{II} in the investigated copper(II) complexes during the catalytic cycle.
(b) The Lewis acidity of the copper(II) center created by nature of the coordinated ligands system.
(c) The geometry imposed by the coordinated ligands on the copper(II) ion.
(d) The degree of liability of the sixth donor atom of the hexa-coordinated complex species. Some of these factors will be considered sequentially.

Geometrical considerations:-

The surprising oxidase like catalytic activity of the inspected coordinatively saturated hexacoordinated copper(II) complexes may be ascribed to conformational changes in solution. The hexa-coordinate complexes are highly unstable in their ground state due to: (a) the excessive build-up of electron density on the central copper(II) ion (six donating atoms), (b) the Jahn–Teller effect. According to the Jahn–Teller theorem, the hexa-coordinated copper(II) complexes are usually associated with a tetragonal distortion reducing the symmetry from O_h to D_h [46]. Consequently we suggest that the axially coordinated counter ion could be forced to get away from the octahedral environment and the coordination number would decrease from six to five. This suggestion find support from the electrical conductivity results in solution (Table 1) which showed that the conductance values of examined complexes are higher than that required for 1:1 electrolytes and lower than that expected for 1:2 electrolytes. Such conformational changes will provide one open site for coordination of the substrate or any reacting species during the oxidation catalytic cycle.

However, the data in Table 7 demonstrate that the five coordinate complexes **4** and **5** exhibit catalytic activity higher than the octahedral halogeno complexes **1** and **2**. The octahedral complexes are coordinately saturated, and thus have no vacant coordination sites, which can be utilized to bind any reacting species during the catalytic process. Due to the reasons (a) and (b) mentioned above, the reported copper(II) chelates should dissociate in solution to form more stable five coordinate complexes with an available coordination site for the substrate binding. The ability of such coordinately saturated complexes to dissociate and consequently the energy of dissociation is one of the key factors in imparting catalytic properties to these complexes. On the other hand, the five coordinate square pyramidal complexes already have a vacant coordination site for the substrate binding and thus need no energy for ligand dissociation as in the case of the octahedral complexes.

However the results here show that octahedral complexes can be effective catalysts and that geometrical effect is only one facet of the complexes activity.

Correlation with the six donor lability:-

Several studies on catechols oxidation demonstrated that, the degree of lability of the axial donor atom has an effect on the rate of catalysis [47]. In addition it has been shown that electron transfer from catechol to copper(II) can begin only after catechol and the copper(II) species form a copper(Il) catecholate intermediate [48]. Our premise is that the ease of dissociation of the sixth coordinated counter anions ligands (X =Cl, Br and NO_3) greatly affects the ability of these hexa-coordinate complexes to catalyze this oxidation process. We assume that prior to oxidation, dissociation of the sixth donor will occur so that a vacant coordination site will be available for the binding of the catechol. Dissociation of the sixth donor counter anion ligand is the spark of the oxidation process so the safe binding of catecholate to copper(II) should be attainable. Therefore, greater the binding ability of the donor counter anion ligand (X) the larger the energy required for the dissociation of the sixth donor X and consequently the slower the reaction will proceed if this step is part of the rate determining step of the reaction. According to the previous studies the coordinating ability of the nitrato ligand is lower than the chloro and bromo ligands. Consequently the lability of the nitrato ligand will be greater than the chloro and bromo donors. This explanation may clarify the superiority of hexacoordinated nitrato complexes as compared with the analogous hexacoordinated halogeno complexes.

When TEA was added to a solution in which the copper(II)-catalyzed oxidation of 3,5-$DTBCH_2$ was in progress, a remarkable increase *ca*. three fold was found in the oxidation rate (Table 7). There is a kinetic factor, which account for this dramatic increase of the catalytic activity on addition of TEA. This marked effect of TEA on the rate of the catalytic oxidation reaction was previously reported for other catechol oxidase functional models catalyze the aerobic oxidation of catechol [49].

Table 7. Catechol oxidase like catalytic activity of copper(II) complexes

*Complex	**3,5-DTBQ × 10^{-2} (m mol L^{-1})	TR × 10^{-1} h^{-1}	3,5-DTBQ× 10^{-2} (m mol L^{-1})	TR × 10^{-1} h^{-1}
1	88.53	147.55	32.36	53.9
2	92.52	154.42	32.68	54.4
3	164.83	274.71	72.57	120.9
4	116.71	194.51	63.17	105.2
5	114.25	190.41	67.48	112.4

*Complex details are as listed in Table 1, **these data are obtained in presence of TEA

Phenoxazinone synthase biomimetic catalytic activity:-

Related to catechol oxidase biomimetic catalytic activity is the ability of the reported copper(II) complexes to promote the oxidation of *o*-aminophenol (OAP) to 2-amino-*3H*-phenoxazine-3-ones (APX) as shown in Figure 4.

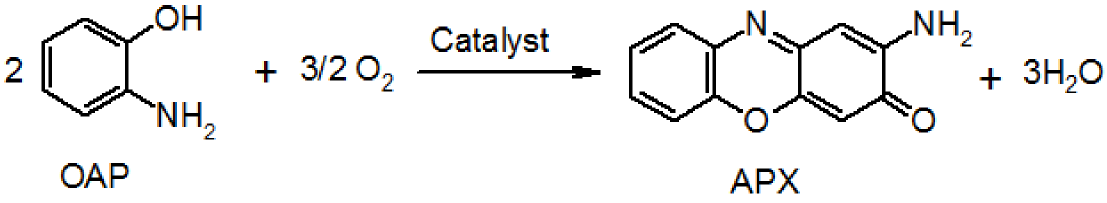

Fig 4: The aerobic catalytic oxidation of *o*-aminophenol (OAP) to 2-amino-*3H*-phenoxazine- 3-ones (APX)

The present series of copper(II) complexes exhibit promising catalytic activity towards the oxidative dehydrogenation of *o*-aminophenol (OAP) at room temperature in the presence of O_2 in methanol. This system can be regarded as a functional model of phenoxazinone synthase which is involved in the biosynthesis of Actinomycin D (AD) a naturally occurring antineoplastic agent from the *o*-aminophenol derivative. The catalytic measurements were carried out by the spectrophotometeric monitoring of the increase in the concentration of the strongly absorbing 2-amino-3*H*-phenoxazin-3-one product (APX) at 433 nm. 2-aminophenol has no absorption in the visible region. The time sequence of the increase in the 400-440 nm band characteristic of the oxidation product (APX) of 2-aminophenol initiated by copper(II) complex **3** at ambient temperature is shown in Figure 5 as a representative of the catalytic aerobic oxidation of (OAP).

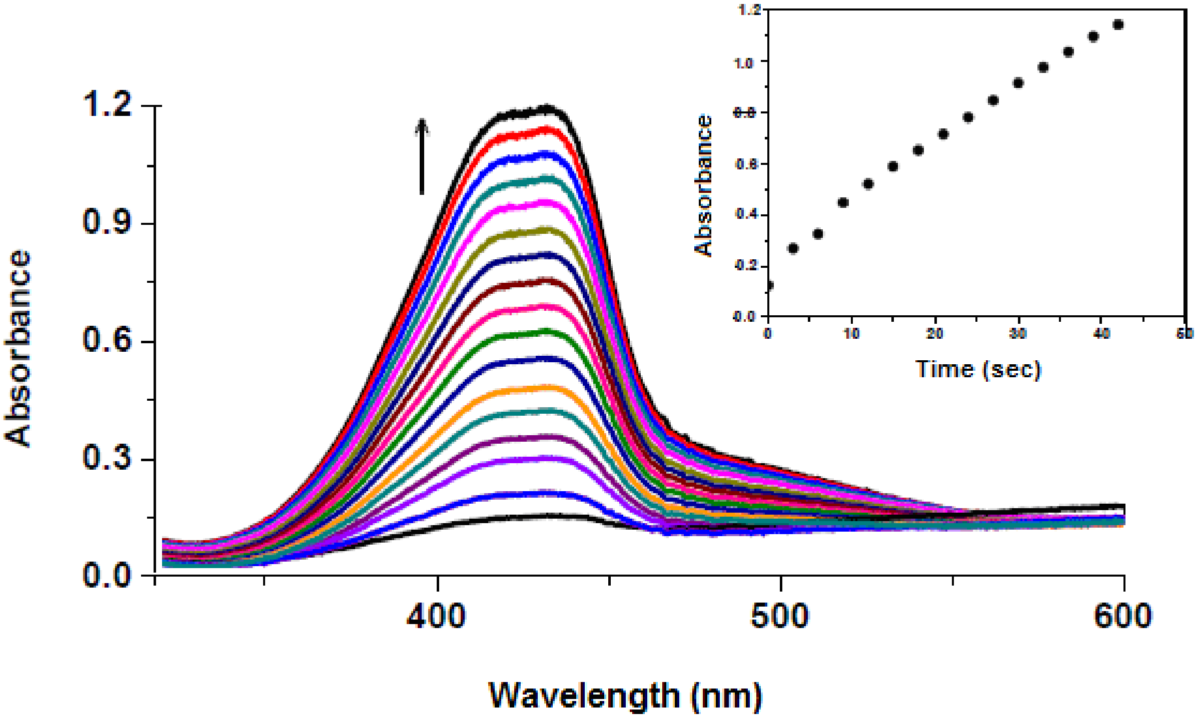

Fig. 5. UV/Vis spectral changes recorded for the reaction of complex (**3**) with 2-aminophenol (0.05 M) in methanol at 296 K; spectrum obtained several milliseconds after mixing of the reactants in the stopped-flow; inset is the kinetic trace at 433 nm

The phenoxazinone synthase biomimetic catalytic activity of the reported copper(II) complexes was evaluated by using the turn over rat TR expiration, (TR = the amount of APX produced per mmole of catalyst per min. (Table 8) by making use of molar absorbance value of 2.23×10^{4} M^{-1} cm^{-1} and the results obtained are presented in Table 8.

Although (APX) is produce for all the synthesized copper(II) chelates, the rate at which it is produced varies from one complex to another. The data in Table 8 demonstrate that, the rate of oxidation of *o*-aminophenol is markedly dependent on both the counter anion incorporeities in the complex molecule and the stereochemistry of the metal chelate. Similar to that reported above for catechol oxidase like activity the candidates copper(II) complexes exhibit the same order of reactivity towards the oxidative dehydrogenation of 2-aminophenol. The observed variation in the catalytic activity of the present copper(II) complexes can be correlated with structural features of the inspected copper(II) chelate. This finding is similar to was reported for catechol oxidase mimetic catalytic activity for the present series of copper(II) complexes.

Similar to the catechol-containing systems a much more dramatic increase (*ca*. 2.88 – 4.28 fold) was found for the oxidation rate when TEA was added to a methanolic solution in which the copper(II) catalyzed oxidation of *o*-aminophenol. In methanol solution *o*-aminophenol is mainly present in its protonated form OAPH. Due to the presence of TEA in the reaction medium, *o*-aminophenol may be predominantly present in the non-protonated form OAP^-. In analogous to catechol, TEA deprotonates OAPH to OAP^-, and the kinetic activity of OAP^- presumably is the spark for initiation of the oxidation catalytic cycle.

Table 8. Phenoxazinone like catalytic activity of copper(II) complexes **1-5**

Complex*	APX (μ mol L^{-1})**	**TR h^{-1}	APX (μ mol L^{-1})	TR h^{-1}
1	84.78	14.13	28.40	4.79
2	77.10	13.00	24.68	3.88
3	137.36	37.79	47.86	9.97
4	99.26	19.54	16.8	5.80
5	125.21	20.74	43.47	7.24

*Complex details are as listed in Table 1; **these data are obtained in presence of TEA. The turn over rate (TR) is the amount of APX produced per min per mg of catalyst.

References:-

1. J. Kaizer, G. Barath, R. Csonka, G. Speier, L. Korecz, A. Rockenbauer, Parkanyi, J. Inorg. Biochem., 102 (2008) 773-780 and references therein.
2. R. Hage, A. Lienke, Angew. Chem., 118 (2006) 212.
3. N. Duran, E. Esposito, Appl. Catal. B, 28 (2000) 83.
4. (a) R.H. Holm, E.I. Solomon, Chem. Rev. 104 (2004) 347; (b) T.C. Harrop, P.K. Mascharak, Acc. Chem. Res. 37 (2004) 253. and references therein; (c) T.S. Lobana, K. Isobe, H. Kitayama, T. Nishioka, I. Kinoshita, Angew. Chem., Int. Engl. 43 (2004) 213; (d) D. Sellmann, R. Prakash, F.W. Heinemann, Eur. J. Inorg. Chem. (2004) 1847; (e) P.A.N. Reddy, B.K. Santra, M. Nethaji, A.R. Chakravarty, J. Inorg. Biochem. 98 (2004) 377; (f) S. Dhar, D. Senapati, P.K. Das, P. Chattopadhyay, M. Nethaji, A.R. Chakravarty, J. Am. Chem. Soc. 125 (2003) 12118; (g) B.K. Santra, P.A.N. Reddy, M. Nethaji, A.R. Chakravarty, J. Chem. Soc., Dalton Trans. (2001) 3553; (h) J.J. Wilker, S.J. Lippard, J. Am. Chem. Soc. 117 (1995) 8682.
5. (a) R.H. Holm, P. Kennepohl, E.I. Solomon, Chem. Rev. 96 (1996) 2239; (b) M.A. Ali, S.M.G. Hossain, S.M.M.H. Majumder, M. Nazimuddin, M.T.H. Tarafder, Polyhedron 6 (1987) 1653.
6. (a) D.T. Minkel, A.L. Saryan, D.H. Petering, Cancer Res. 38 (1978) 124; (b) D.T. Minkel, C.H. ChanStier, D.H. Petering, Mol. Pharmacol. 12 (1976) 1036; (c) C.H. ChanStier, D.T. Minkel, D.H. Petering, Bioinorg. Chem. 5 (1976) 203.
7. W. Kamin and B. Schwederski, *Bioinorganic Chemistry: Inorganic Elements in the Chemistry of Life,* Wiley, 1st Edit., New York, (1995), Ch 10, and references therein.
8. M. Termoliere and J. B. Bieth, *Photochemistry,* **23,** 501 (1983)
9. F. Zippel, H. F. Nolting, B. Kerbs and H. Witzel, *J. Inorg. Biochem.,* **59,** 715 (1995).
10. Z. Tyeklar, K. D. Karlin, *Acc. Chem. Res.,* **22,** 241, (1989); N. Kitajima, K. Fujisama, H. Moro-Oka and J. K. Touriumi, *J. Am. Chem. Soc.,* **111,** 8975 (1993); D. Bockcliffe and A. E. Martell, *Inorg. Chem.,* **32,** 3143 (1993) and references therein; M. R. Malachowski and M. G. Davidson, *Inorg. Chim. Acta,* **162,** 199 (1989); E. Spodine and J. Manzur, *Cood. Chem. Rev.,* **119,** 171 (1992); E. I. Solomon, *Chem. Rev.,* **94,** 827 (1994)
11. S. Kida, H. Okawa and Y. Nishida, *Copper Coordination Chemistry: Biochemical and Inorganic Perspectives,*Adenine, Guilderland, New York, (1989), pp 259, 425.
12. A. Oikawa, *Biochemistry. Jpn,* **48,** 872 (1976); G.A. Swan, *J. Chem. Soc.,Perkin II,* **1977,** 1346 (1977); S. A. Burchill, R. Virden and A. J. Thody, *J. Invest. Dermatol.,* **93,** 236 (1989); P. Peechurm, S. A. Burchill and A. J. Thody, *J.*

Endocrinol, **119,** 517 (1988); V. J. Hearing and M. Jimerez, *Int. J. Biochem.*, **19,** 1141 (1987); G. Prota, *Prog. Clin. Biol. Res.*,**256,** 101 (1988).

13. C. E. Barry, P.G. Nayar, T.P. Begley, Biochem. 28 (1989) 6323.
14. G.H. Jones, D.A. Hopwood, J. Biological Chem. 259 (1984) 14151
15. a) R.F. Cunico, and R.K. Pandey, J. Org. Chem., 70, (2005) 5344; b) M. Carmack, and A. P. Komin, J Heterocyclic Chem., 13, (1976**)**13; c) P.G. Baraldi, J.J. Diaz-MochÓn, A. Espinosa, M. A. Gallo, M.J. Pineda-de-Las-Infantas, R. Romagnoli, and A. Unciti-Broceta, J.Org. Chem. 70, (2005) 2878-2880
16. W.J. Geary, Coord. Chem. Rev. **7** (1971) 81.
17. A.W. Coats, J.P. Redfern, Nature, 201, (1964) 68.
18. K. Nakamoto, Infrared and Raman Spectra of Inorganic and Coordination Compounds, Wiley, New York, 1986.
19. W. Radecka-Paryzek, V. Patroniak-Krzyminiewska, H. Litkowska, Polyhedron 17 (1998) 1477.
20. R. M. El-Shazly, G. A. A. El-Hazmi, S. E. Ghazy, El-Shahawi M S, A. A. El-Shamy,.Spectrochem. Acta A 61 (2005) 243.
21. A. Kumar, G. Singh, K. Singh, R N Handa, S. N. Dubey, Proc. Acad. Sci. 72A, **11**, (2002) 87.
22. N.F. Curtis, Y.E.M. Curtis, Inorg. Chem. **4** (1965) 804.
23. A. M. Ramadan, M. M. El-Naggar, *J. Inorg. Biochem*., **63**, (1996) 143.
24. K. Nakamoto, Infrared and Raman Spectra of Inorganic and Coordination Compounds, Wiley, New York, 1986.
25. D.A. Waldwin, A.B.P. Lever, R.V. Parish, Inorg. Chem. **10** (1971) 107.
26. Y.J. Seok, K.S. Yang, S.T. Kim, W.K. Huh, S.O. Kang, J Carbohydrate Chemistry **15** (1996) 1085.
27. M. J. MacLachlan, M.K. Park, L.K. Thompson. Inorganic Chemistry, **35** (1996) 5492-5499.
28. a) M.M.H. Khalil, M. M. Aboaly, R. M. Ramadan. Spectrochimica Acta Part A, 61 (2005) 157; b) O.A.M. Ali, M.M.H. Khalil, G.M. Attia, R.M. Ramadan. Spectroscopy Letters, **36** (2003) 71.
29. a) M. M. H. Khalil, S. A. Ali, R. M. Ramadan. Spectrochimica Acta 57A (2001) 1017-1024; b) B.P. Straughan, S. Walker, Spectroscopy, vol. 1, John Wiley & Sons, Inc., USA, 1976.
30. a) M. Akbar Ali, A.H. Mirza, M. Nazimuddin, H. Rahman, R.J. Butcher, Polyhedron **20** (2001) 2431; (b) A.G. Bingham, H. Bogge, A. Muller, E.W. Ainscough, A.M. Brodie, J. Chem. Soc., Dalton Trans. (1987) 493; (c) E.W. Ainscough, A.M. Brodie, J.D. Ranford, J.M. Waters, J. Chem. Soc., Dalton Trans. (1991) 2125.
31. A. D. Harrish, B. Josses, R.D. Archer, Inorg Chem., **4** (1965) 147-149.
32. A.B.P. Lever. Inorganic Electronic Spectroscopy, 2nd ed.; Elsevier: New York, 1984.
33. O.O.E. Onawumi, O.O.P. Faboya, O.A. Odunola, T.K. Prasad, M.V. Pajasekharan, Polyhedron **27** (2008) 113.
34. a) R.N. Patel, N. Singh, D.K. Patel, V.L.N. Gundla, Indian J. Chem. 46A (2007) 422; b) N.M. El-Metwaly, I. M. Gabr, A.A. El-Asmy, Trans. Met. Chem. **31** (2006) 71; c) K. Singh, M.S. Barwa, P. Tyagi, Eur. J. Med. Chem. **42** (2007) 394; d) Y. Li, C. Yan, Z. Wu, C. Zhu, J. Mag. Mag. Mater. **292** (2005) 418.
35. B. N. Figgis, J. Lewis, *Prog. Inorg. Chem*., **6**, (1964) 37.
36. R. L. Dutta, A. Syamal, *Elements of Magnetochemistry*, second Ed., Affiliated East-West Press, Delhi, (2007).
37. R.C. Aggarwal, N.K. Singh, R.P. Singh, Inorg. Chem. **20** (1981) 2794.
38. M.J. Bew, B.J. Hathaway, R.R. Fereday. J Chem. Soc., Dalton Trans, (1972) 1229-1237.
39. J.E. Wertz, J.R. Bolton. Electron Spin Resonance, McGraw. Hill Book Company, New York, 1972.
40. D. Kivelson, R. Neiman. Journal of Chemical Physics, **35** (1961) 149.
41. B. J. Hathaway, A. A. Tomlinson, Coord. Chem. Rev. **5** (1970) 1.
42. a) B. J. Hathaway, D. E. Billing, Coord. Chem. Rev. **5**: (1970) 143; b) B. J. Hathaway, R. J. Dudley, P. Nicholls, J. Chem. Soc. A (1968) 1845; c) R. J. Dudley, B. J. Hathaway, J. Chem. Soc. A (1970) 1725.
43. B.J. Hathway, Coord. Chem. Rev., **52** (1983) 87.
44. a) E. I. Solomon, U. M. Sundaram and T. E. Machonkin, Chem. Rev.,96 (1996) 2563.; (b) R. Than, A. A. Feldmann and B. Kerbs, Coord. Chem. Rev. **182** (1999) 211; (c) C. Gerdemann, Ch. Eicken and B. Kerbs, Acc. Chem. Res. (2002) 183; (d) C. X. Zhang, H. C. Liang, K. J. Humphreys, K. D. Karlin, in: L. I. Simandi (Ed), Advanced in Catalytic Activation of Dioxygen by Metal Complexes, Kluwer Academic Publishers, Dordrecht (2003) 79; (e) M. U. Triller, D. Pursches, W. Y. Hsieh, V. L. Pecoraro, A. Rompel and B. Kerbs, Inorg. Chem. **42** (2003) 6274.; (f)V. L. Pecoraro, M. J. Baldwin and A. Gelasco, Chem. Rev., **94** (1994) 807.; (g) A. J. Wu, J. E. Penner-Hahn and V. L. Pecoraro, Chem. Rev.,104 (2004) 903.; P. Gentschev, N. Moller and B. Kerbs, Inorg. Chim. Acta, **300** (2000) 442.; (h) R. Wegner, M. Gottschaldat, H. Gorls, E. –G. Jager and D. Klemm, Chim. Eur. J. **7** (2001) 2143.
45. a) T. Funabiki, in: L. I. Simandi (Ed), Advanced in Catalytic Activation of Dioxygen by Metal Complexes, Kluwer Academic Publishers, Dordrecht, (2003) 157.; (b) T. Funabiki, H. Sakamoto, S. Yoshida and K. Tarama, J. Chem. Soc., Chem. Commun, (1979) 754.; (c) C. Fernandes, A. Neves, A. G. Bortoluzzi, A. S. MangrichE. Rentschler, B. Spoganicz and E. Schwingel, Inorg. Chim. Acta. **12** (2001) 320.; (d) S. Mukherjee,

T. Weyhermuller, E. Bothe, K. Wieghardt and P. Chaudhuri, Dalton Trans. (2004) 3842.; (e) P. Chaudhuri, Coord. Chem. Rev. **243** (2003) 143; (f) M. Costas, M. P. Mehn, M. P. Jensen and L. Que, Chem. Rev. **104** (2004) 939.

46. A. Hudson, J. Mol. Phys., **10** (1966) 575; I. B. Bersuker, Coord. Chem. Rev., **14**, 357 (1975).
47. a) M. R. Malachowski, B. T. Dorsey, M. J. Parker, M. E. Adams and R. S. Kelly, Polyhedron, **17**, .8, (1998) 1289; b) M. R. Malachowski, B. Dorsey, J. G. Sackett, R. S. Kelly, A. L. Ferko, R. N. Hardin, Inorg. Chim. Acta, **249** (1996) 85; c) M. R Malachowski, L. J. Tomlinson, M. G. Davidson, M. J. Hall, J. Coord. Chem., **25** (1992) 171.
48. J.M.M. Rogic, M.D. Swerdloff, T.R. Demmin, K.D. Karlin, J. Zubieta (Eds.), Copper Coordination Chemistry: Biochemical and Inorganic Perspectives, Adenine, Guilderland, NY, (1983) 167.
49. A. M. Ramadan, M. M. Ibrahim, I. M. El-Mehasseb, J Coord Chem. **65**,13, (2012) 2256–2279